Infect Chemother. 2021 Dec;53(4):730-740
https://doi.org/10.3947/ic.2021.0111
pISSN 2093-2340·eISSN 2092-6448

Infection & Chemotherapy

Original Article

Check for updates

Effective Antiviral Activity of the Tyrosine Kinase Inhibitor Sunitinib Malate against Zika Virus

Chen-Sheng Lin [1], Su-Hua Huang [2], Bo-Yu Yan[3], Hsueh-Chou Lai [4], and Cheng-Wen Lin [2,3]

[1]Division of Gastroenterology, Kuang Tien General Hospital, Taichung, Taiwan
[2]Department of Medical Laboratory Science and Biotechnology, Asia University, Taichung, Taiwan
[3]Department of Medical Laboratory Science and Biotechnology, China Medical University, Taichung, Taiwan
[4]Division of Hepato-Gastroenterology, Department of Internal Medicine, China Medical University Hospital, Taichung, Taiwan

OPEN ACCESS

Received: Sep 30, 2021
Accepted: Nov 11, 2021

Corresponding Author:
Cheng-Wen Lin, PhD
Department of Medical Laboratory Science and Biotechnology, China Medical University, No. 100, Sec. 1, Jingmao Rd., Beitun Dist., Taichung City 406040, Taiwan.
Tel: +886-4-22053366 ext 7210
Fax: +886-4-22057414
E-mail: cwlin@mail.cmu.edu.tw

ORCID iDs
Chen-Sheng Lin
https://orcid.org/0000-0003-4450-1125
Su-Hua Huang
https://orcid.org/0000-0002-3453-6052
Hsueh-Chou Lai
https://orcid.org/0000-0002-0126-6447
Cheng-Wen Lin
https://orcid.org/0000-0003-0165-2652

Funding
This work was financially supported by China Medical University, Taiwan (CMU109-ASIA-07, CMU109-MF-57, CMU109-S-09), and funded

ABSTRACT

Introduction: Zika virus (ZIKV), a mosquito-borne flavivirus, causes the outbreaks of Latin America in 2015 - 2016, with the incidence of neurological complications. Sunitinib malate, an orally bioavailable malate salt of the tyrosine kinase inhibitor, is suggested as a broad-spectrum antiviral agent against emerging viruses like severe acute respiratory syndrome coronavirus (SARS-CoV) and SARS-CoV-2.
Materials and Methods: This study investigated the antiviral efficacy and antiviral mechanisms of sunitinib malate against ZIKV infection using cytopathic effect reduction, virus yield, and time-of-addition assays.
Results: Sunitinib malate concentration-dependently reduced ZIKV-induced cytopathic effect, the expression of viral proteins, and ZIKV yield in supernatant with 50% inhibitory concentration (IC_{50}) value of 0.015 μM, and the selectivity index of greater than 100 against ZIKV infection, respectively. Sunitinib malate had multiple antiviral actions during entry and post-entry stages of ZIKV replication. Sunitinib malate treatment at entry stage significantly reduced the levels of ZIKV RNA replication with the reduction of (+) RNA to (-) RNA ratio and the production of new intracellular infectious particles in infected cells. The treatment at post-entry stage caused a concentration-dependent increase in the levels of ZIKV (+) RNA and (-) RNA in infected cells, along with enlarging the ratio of (+) RNA to (-) RNA, but caused a pointed increase in the titer of intracellular infectious particles by 0.01 and 0.1 μM, and a substantial decrease in the titer of intracellular infectious particles by 1 μM.
Conclusion: The study discovered the antiviral actions of sunitinib malate against ZIKV infection, demonstrating a repurposed, host-targeted approach to identify potential antiviral drugs for treating emerging and global viral diseases.

Keywords: Zika Virus; Sunitinib; Antiviral agents; Inhibitory concentration 50; Protein kinase inhibitors

INTRODUCTION

Zika virus (ZIKV) is one of medically important mosquito-borne flaviviruses, as the agents of sexually transmitted diseases in the family *Flaviviridae* [1, 2]. ZIKV, firstly detected in Uganda

by grants from the Ministry of Science and Technology, Taiwan (MOST108-2320-B-039-039-MY3, MOST110-2923-B-039-001-MY3). The experiments and data analysis were performed in part using the Medical Research Core Facilities Center, Office of Research & Development at China Medical University, Taiwan.

Conflict of Interest

No conflicts of interest.

Author Contributions

Conceptualization: CSL, HCL, CWL. Data curation: CSL, SHH, BYY. Formal analysis: CSL, SHH, BYY, CWL. Funding acquisition: HCL, CWL. Investigation: CSL, HCL, CWL. Methodology: CSL, CWL. Project administration: CSL, HCL, CWL. Resources: CWL. Software: HCL, CWL. Supervision: CWL. Validation: SHH, BYY, HCL. Visualization: CWL. Writing - original draft: CSL, HCL, CWL. Writing - review & editing: CSL, SHH, BYY, HCL, CWL.

in 1947, appears outside the equatorial zone across Africa and Asia since 2007, such as in Yap Island in 2007, in French Polynesia in 2013 - 2014, in Latin America in 2015, and in North America in 2016. ZIKV primarily causes mild diseases, including fever, rash, exanthema, jaundice, arthralgia, and conjunctivitis [3, 4]. In the outbreaks of Latin America in 2015 - 2016, ZIKV infection has been reported to correlates with the incidence of neurological complications, such as Guillain-Barré syndrome, newborn infants with microcephaly, fetal abnormalities, and pregnancy losses with birth defects [5]. Due to the association of fetal microcephaly with ZIKV infection, the World Health Organization announces a “public health emergency of international concern” in 2016 [6]. Nowadays, ZIKV is still broadly circulating in the Southeast Asia, the Pacific Islands, and Americas, potentially spreading to the rest of the world [7, 8]. Therefore, the vaccines or antiviral treatments are the urge to prevent ZIKV infection and cure the patients, leading to diminish the cases with fetal microcephaly and abnormalities.

ZIKV RNA genome with near 11 kb in length encodes a unique long open reading frame consisting of C, prM, E, NS1, NS2a, NS2b, NS3, NS4a, NS4b, and NS5 proteins [1, 9]. The E protein interacts with host attachment factors and receptors, as the determinant of virus tropism and virulence [1, 9]. ZIKV NS3 protein contains a serine protease domain at the N-terminus and a helicase domain at the C-terminus, displaying the protease activity with the cofactor NS2B. NS5 has a C-terminal RNA-dependent RNA polymerase (RdRp) and a N-terminal methyltransferase (MTase) activity, involving in viral genome replication [1, 9]. These essential ZIKV proteins have been suggested as the targets for developing anti-ZIKV agents. The synthetic peptide inhibitor, Z2, specifically interacts with ZIKV E protein, reducing the viral entry [10]. Novobiocin, lopinavir-ritonavir and bromocriptine show the inhibitory effect on the proteolytic activity of ZIKV NS2B-NS3 protease [11, 12]. In addition, fidaxomicin directly interacts with ZIKV NS5 protein, inhibiting the RNA synthesis-catalyzing activity of ZIKV RdRp [13]. However, potently effective therapeutics of ZIKV infection are not currently available. Identifying anti-ZIKV compounds is instantly desired.

Sunitinib malate, an orally bioavailable malate salt of the tyrosine kinase inhibitor, significantly inhibits the multi-specific tyrosine kinase receptors such vascular endothelial growth factor receptor 2 (VEGFR2), platelet-derived growth factor receptor b (PDGFRb), and c-kit [14]. Sunitinib malate has been approved to treat renal cell carcinoma and gastrointestinal stromal tumors [14]. Since many viruses capture a lot of host kinases during viral replication, approved kinase inhibitors have been repurposed as host-targeted broad-spectrum antiviral therapies [15]. Erlotinib, gefitinib, and lapatinib (anticancer drugs targeting EGFR and ERBb kinase family ERBB2) demonstrate *in vitro* and *in vivo* antiviral activities against hepatitis C virus (HCV) and human cytomegalovirus [16, 17]. Imatinib and nilotinib (approved anticancer c-Abl inhibitors) significantly inhibit replication of Ebola virus [18], dengue virus (DENV) [19], Middle East Respiratory Syndrome coronavirus (MERS-CoV), and severe acute respiratory syndrome (SARS)-CoV [20] in cultured cells. Interestingly, sunitinib shows the meaningful suppression on *in vitro* and *in vivo* replication of DENV and Ebola virus [21]. Recent, kinase inhibitors of anticancer drugs, including sunitinib malate, have been repurposed as the treatment of coronavirus disease 2019 (COVID-19), due to the antiviral potential with inhibitory potency on the key kinases for viral entry and reproduction [22]. Meanwhile, sunitinib malate, inhibiting AP2M1 phosphorylation, markedly impeded the entry stage of SARS-CoV-2 pseudoviruses [23]. Previous studies indicate that sunitinib might be a broad-spectrum inhibitor against DNA and RNA enveloped viruses.

This study investigated the antiviral efficacy of sunitinib malate against ZIKV infection on cytopathic effect, viral protein and RNA genome synthesis, and virus yield. The study provided the antiviral potency and the mechanism of action by sunitinib malate against ZIKV.

MATERIALS AND METHODS

1. Cell viability assay

The effect of sunitinib malate (Sigma, Darmstadt, Germany) on cell viability of baby hamster kidney (BHK)-21 cells (Bioresource Collection and Research Center, Hsinchu, Taiwan) was measured by 3-(4,5-dimethylthiazol-2-yl)-2,5-diphenyltetrazolium bromide (MTT) assay. 2×10^3 BHK-21 cells/well cultured in 96-well plates were treated with sunitinib malate at the concentrations of 0, 0.01, 0.1, 1, 5, and 10 μM, respectively. After a 96-h treatment, the treated cells were incubated with 20 μl of MTT stock solution for 4 h, and then added 100 μl of dimethyl sulfoxide in each well for an additional 1-h incubation. The formazan product was determined by the SpectraMax® iD3 Multi-Mode Microplate Reader (Molecular Devices, Winooski, VT, USA) with the absorbance of optical density at 570 and 630 nm ($OD_{570-630}$). Cell viability (%) was calculated as {($OD_{570-630}$ of treated cells - $OD_{570-630}$ of blank control) / ($OD_{570-630}$ of mock-treated cells - $OD_{570-630}$ of blank control)} × 100. Cytotoxic concentration giving 50% (CC_{50}) was calculated by linear regression curve program.

2. Inhibitory assays of cytopathic effect reduction and viral protein synthesis

To examine the antiviral activity of sunitinib malate against ZIKV, cytopathic effect and apoptosis (sub-G1 fraction) of ZIKV-infected cells with or without the treatment of sunitinib malate were detected using microscopic photograph and flow cytometry cell cycle analysis by propidium iodide (PI) staining. BHK-21 cells grown in Minimum Essential Media (MEM) containing 2% FBS were infected with ZIKV strain $PRVABC_{59}$ kindly provided by Professor Robert Y.-L. Wang of Chang Gung University at a multiplicity of infection (MOI) of 0.05, and immediately treated with sunitinib malate (0, 0.01, 0.1, and 1 μM). After a 4-day incubation, infected/treat cells were photographed by an inverted microscope for examining the levels of ZIKV-induced cytopathic effect. In addition, the production of viral E protein expression in the infected/treat cells were analyzed by the immunofluorescence assay (IFA) with rabbit anti-ZIKV-E (GeneTex, Inc, Irvine, CA, USA) and anti-rabbit IgG antibodies conjugated with AF555 (ThermoFisher, Waltham, MA, USA), then relative fluorescence intensity of stained ZIKV E protein was counted in mock and treated infected cells transfected cells by Image J software. In the flow cytometry cell cycle assay, the cells were harvested, washed, fixed, and then stained using the PI solution for 15 min in the dark. The cell cycle profile of beyond 10,000 cells per sample was directly analyzed by flow cytometry with an excitation wavelength of 488 nm and the emission wavelength of 620 nm, as described in our prior report [24].

3. Virus yield inhibitory assay

To test the inhibitory effect of sunitinib malate on the virus yield in ZIKV-infected cells, BHK-21 cells plated in 6-well plates were infected with ZIKV at an MOI of 0.05, and immediately treated with sunitinib malate (0, 0.01, 0.1, and 1 μM). After a 96-h incubation, cultured supernatant from each group of infected/treated cells was collected, and then serially diluted and added onto the cells in 96-well plates for measuring virus yields by the median tissue culture infectious dose ($TCID_{50}$) assay. The cells of each well were classified as infected or not infected based on the cytopathic effects (CPE) upon infection with ZIKA 96 h post the inoculation with the diluted solutions. The dilution exhibiting 50% of the wells with a CPE

https://doi.org/10.3947/ic.2021.0111

was determined as the $TCID_{50}$ of the cultured supernatant, which virus yield was presented as $TCID_{50}$/ml. The 50% inhibitory concentration (IC_{50}) value of sunitinib malate on reducing 50% virus yield was calculated according to the inhibitory activity at the concentrations of 0.01, 0.1, and 1 μM using linear regression curve program. Also, the selective index (SI) was assessed by the ratio of CC_{50} to IC_{50}.

4. Time-of-addition/removal assays with entry and post-entry stage modes

The time-of-addition/removal assays comprised two modes of co-treatment/removal (entry-stage) and post-infection treatment/removal (post-entry stage) modes. In the entry mode, the cells were co-treated with sunitinib malate (0, 0.01, 0.1, and 1 μM) and ZIKV (MOI = 0.05) for 1 h, washed twice using phosphate-buffered saline (PBS), and further incubated for 120 h. The supernatant from each well was harvested for detecting the virus yield using the $TCID_{50}$ assay, described above. In the post-entry mode, the cells were infected ZIKV for 1 hour, washed twice with PBS, treated with effective sunitinib malate for an additional 1 h, washed again, and then cultured for 120 h. Virus yield in the supernatant collected from each well was also determined by the $TCID_{50}$ assay. The IC_{50} value of sunitinib malate at the entry and post-entry stages was calculated based on reducing 50% virus yield using linear regression curve program.

5. Quantitative assays of ZIKV positive- and negative-strand RNA genomes and intracellular infectious viral particles

For determining anti-ZKIV activity of sunitinib malate on the product of intracellular infectious particles and the synthesis of viral RNA genome, the infected/treated cells under the entry and post-entry stages were harvested 36 h post incubation for measuring relative ZIKV positive- strand RNA genomes and negative-strand replicative RNA intermediates. Total RNAs of the infected/treated cells were extracted using PureLink Mini Total RNA Purification Kit (ThermoFisher) 36 h post treatment, reverse-transcripted with ZIKV RNA-specific capture primers 5'-GTTGAGGGTTTCCACTCTTG-3' for positive-strand RNA genomes and 5'-ACCCTGGGATGTGGTG -3' for negative-sense replicative RNA intermediates, respectively. The assay was further followed by measuring ZIKV positive-strand RNA genomes using SYBR Green Master Mix kit with NS5-specific primer pairs (5'-CTTGTGGCTGCTGCGGAGGTCA-3' and 5'-GTGGTGGGAGCAAAACGGAACTT-3') by 7300 Realtime PCR system (Applied Biosystems, Foster City, CA, USA). The corresponding threshold cycle value (C_t) measured was determined the relative levels of positive- and negative- strand RNA genomes in (un-) treated infected cells were determined by real-time RT-PCR assay normalized by the housekeeping gene GAPDH, described in our prior report [25]. In addition, the infected/treated cells were harvested 72 h post incubation for assessing intracellular infectious viral particles, and then lysed through three freeze-thaw cycles. Each 10-fold serial dilution of the lysate was added into 8 wells in the 96-well plate of BHK-21 cell culture, incubated for 120 h, and the $TCID_{50}$ titer of intracellular infectious viruses was computed, as mentioned above.

6. Statistical analysis

All data of three independent experiments were calculated using One-way ANOVA and Scheffe's post-hoc test by SPSS 12.0 (SPSS, Inc., IBM, Chicago, IL, USA). P <0.05 was considered as a statistically significant result.

https://doi.org/10.3947/ic.2021.0111

RESULTS

1. Antiviral activity of sunitinib malate against ZIKV

Initially, the cytotoxicity of sunitinib malate to BHK-21 cells was firstly evaluated using MTT assays for determining the optimal test concentrations with less cytotoxicity. The CC_{50} value of sunitinib malate to BHK-21 cells was 1.7 μM, thus sunitinib malate at the concentrations of 0.01, 0.1, and 1 μM was used for subsequent antiviral assays, including CPE inhibition, viral protein synthesis, apoptosis reduction, and virus yield tests (**Figs. 1**, **2**). In the CPE inhibition assay, microscopic photography indicated that sunitinib malate concentration-dependently reduced ZIKV-induced CPE in BHK-21 cells (**Fig. 1A**_top). Immunofluorescence images of cells stained with anti-ZIKV E antibodies demonstrated that sunitinib malate inhibited viral E protein expression in ZIKV infected cells by concentration-dependent manners (**Fig. 1A**_bottom, 1B). Meanwhile, apoptotic cell fraction of infected cells treated with or without sunitinib malate was measured using PI staining and flow cytometric assay (**Fig. 2A**). ZIKV-infected cell had the appearance of a sub-G1 (apoptotic) fraction, but sunitinib malate significantly diminished the sub-G1 fraction of ZIKV-infected cells. Moreover, the $TCID_{50}$ assay of supernatant virus yield demonstrated that sunitinib malate markedly inhibited the production of ZIKV in BHK-21 cells (**Fig. 2B**). The IC_{50} value of sunitinib malate on virus yield was 0.015 ± 0.002 μM (**Fig. 2B**). The

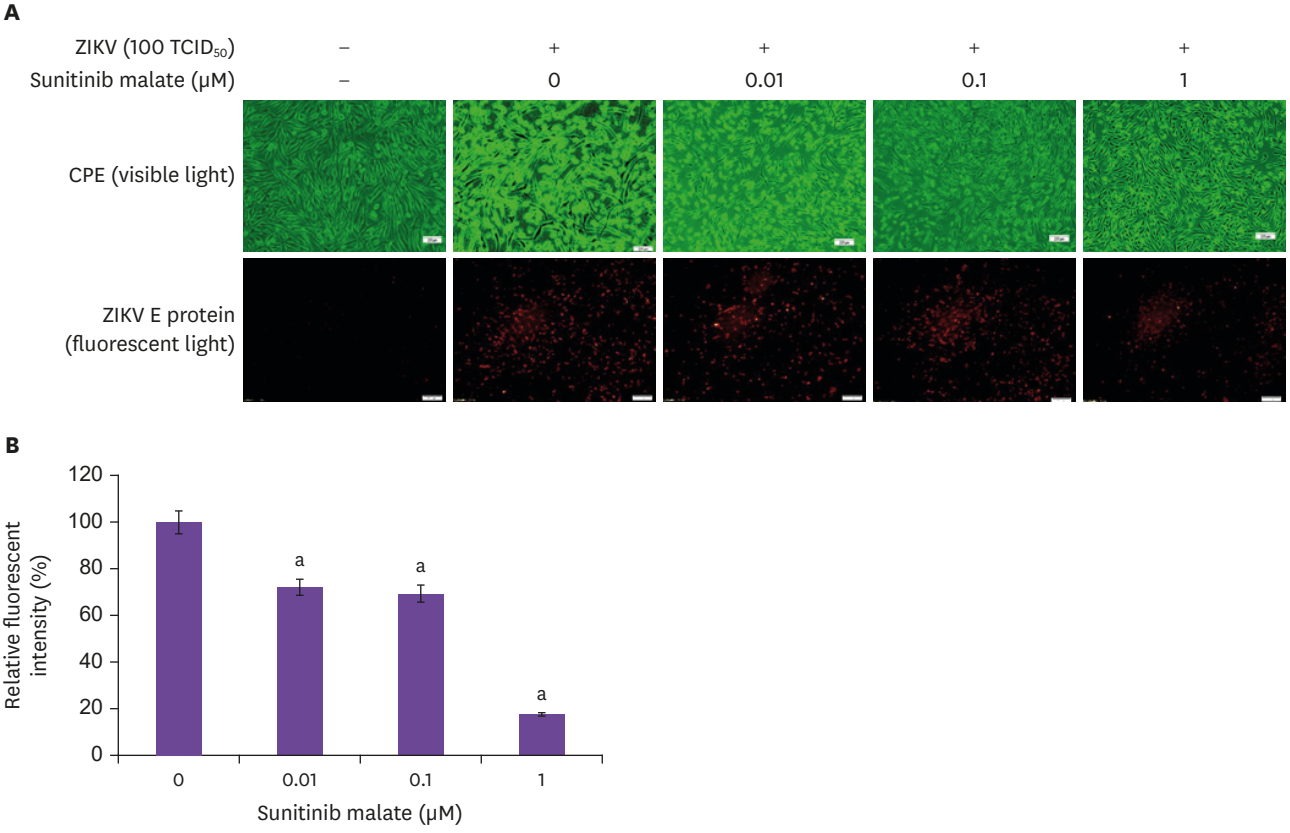

Figure 1. Inhibition effect of sunitinib malate on ZIKV strain $PRVABC_{59}$-induced cytopathic effects and viral E protein expression in BHK-21 cells.
The cells were infected with ZIKV strain $PRVABC_{59}$ at an MOI of 0.05 and immediately treated with sunitinib malate at the indicated concentrations. Images of ZIKV-induced cytopathic effects were photographed 96 hpi (hours post-infection) by phase-contrast microscopy (A, top). Then, the treated/infected cells were assayed using immunofluorescence staining with anti-ZIKV E antibodies and secondary antibodies conjugated with AF555 (A, bottom). Moreover, relative fluorescence intensity of stained ZIKV E protein was counted in mock and treated infected cells transfected cells by Image J software (B).
[a]*P*-value <0.001 compared with un-treated infected cells. Scale bar, 100 μm.
ZIKV, Zika virus; BHK, baby hamster kidney; MOI, multiplicity of infection; TCID, tissue culture infectious dose; CPE, cytopathic effects.

https://doi.org/10.3947/ic.2021.0111

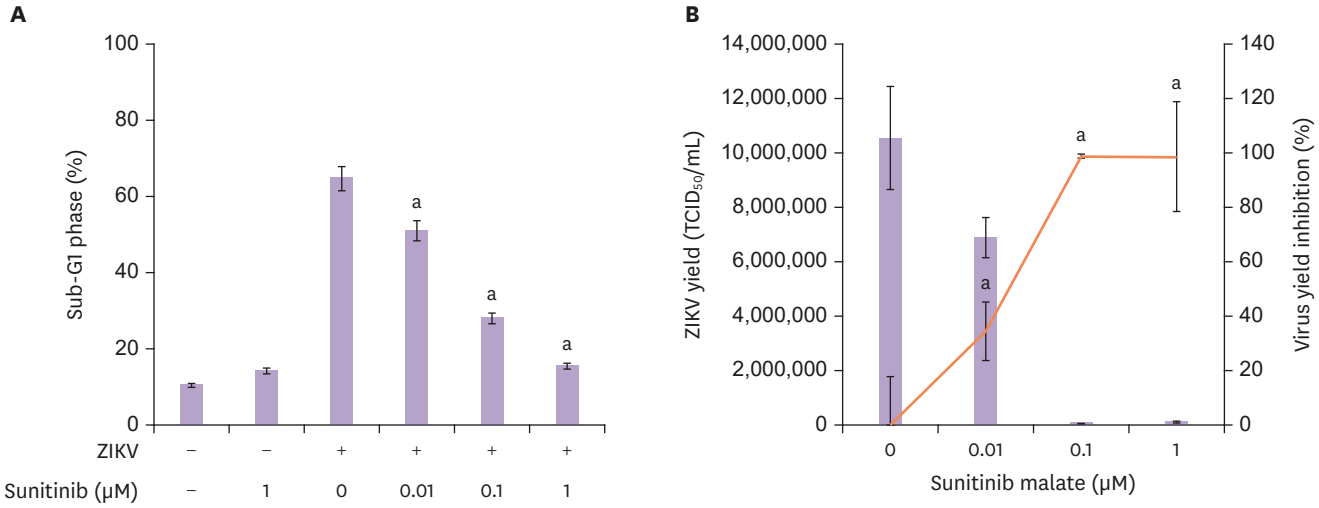

Figure 2. Inhibitory effect of sunitinib malate on ZIKV strain $PRVABC_{59}$-induced sub-G1 phase and virus yield in BHK-21 cells.
The cells were infected with ZIKV strain $PRVABC_{59}$ at an MOI of 0.05 and immediately treated with sunitinib malate at the indicated concentrations. Mock and infected cells treated with or without sunitinib malate were harvested 96 hpi, stained using propidium iodide, and then examined using flow cytometry. The percentage of sub-G1 phase in treated/infected cells was displayed (A). The supernatant from treated infected cells was harvested 96 hpi and serially diluted for determining virus yield using the $TCID_{50}$ assay (B, left y axis). The rate of virus yield inhibition was calculated based on the ratio of the loss in the titer of the treated group to un-treated group (B, right y axis).
[a]*P*-value <0.001 compared with un-treated infected cells.
ZIKV, Zika virus; BHK, baby hamster kidney; MOI, multiplicity of infection; TCID, tissue culture infectious dose.

selectivity index (IC_{50}/CC_{50}) of sunitinib malate against ZIKV infection was 113, discovering that sunitinib malate was a selective active agent for treating ZIKV diseases.

2. The mechanisms of anti-ZIKV action by sunitinib malate

To ascertain antiviral mechanism(s) of sunitinib malate on the stages of ZIKV replication cycle, the antiviral action of sunitinib malate was further evaluated using time-of-addition/removal assays including two modes of co-treatment/removal (entry-stage) and post-infection treatment/removal (post-entry stage) modes. After a 1-h incubation of the virus/the compound mixture in the cultured wells, the cell monolayer was washed with PBS, followed an additional 120-h incubation, and then harvested the supernatant for determining virus yield in untreated and treated infected cells using the $TCID_{50}$ assay (**Fig. 3**). Profiles of the ZIKV yield revealed that sunitinib malate concentration-dependently inhibited both entry and post-entry stages of ZIKV replication in vitro (**Fig. 3**), while the IC_{50} values of sunitinib malate on ZIKV yield were 0.011 ± 0.002 μM at entry stage, and 0.009 ± 0.001 μM at post-entry stage, respectively. Results demonstrated that sunitinib malate had a potent inhibitory activity on the entry and post-entry stages during the ZIKV replication.

To examine the inhibitory action of sunitinib malate on ZIKV RNA replication, the infected cells treated at entry or post-entry stage were washed, incubated for 36 h, and then harvested for real-time RT-PCR analysis of intracellular ZIKV positive-strand RNA genomes [(+) RNA] and negative-sense replicative RNA intermediates [(-) RNA] (**Fig. 4**). Relative levels of (+) RNA and (-) RNA by real-time RT-PCR with the specific capture primers indicated that the copies of positive-sense RNA genomes and negative-sense replicative RNA intermediates in infected cell treated at entry stage was lower than those in infected cell treated at post-entry stage, as correlated with a larger amount of intracellular ZIKV at post-entry stage (a 2-h incubation with virus) than the entry stage (one-hour incubation with virus) (**Fig. 4A**, **4B**, **4D**, **4E**). The ratio of (+) RNA to (-) RNA discovered that sunitinib malate treatment at entry stage significantly

https://doi.org/10.3947/ic.2021.0111

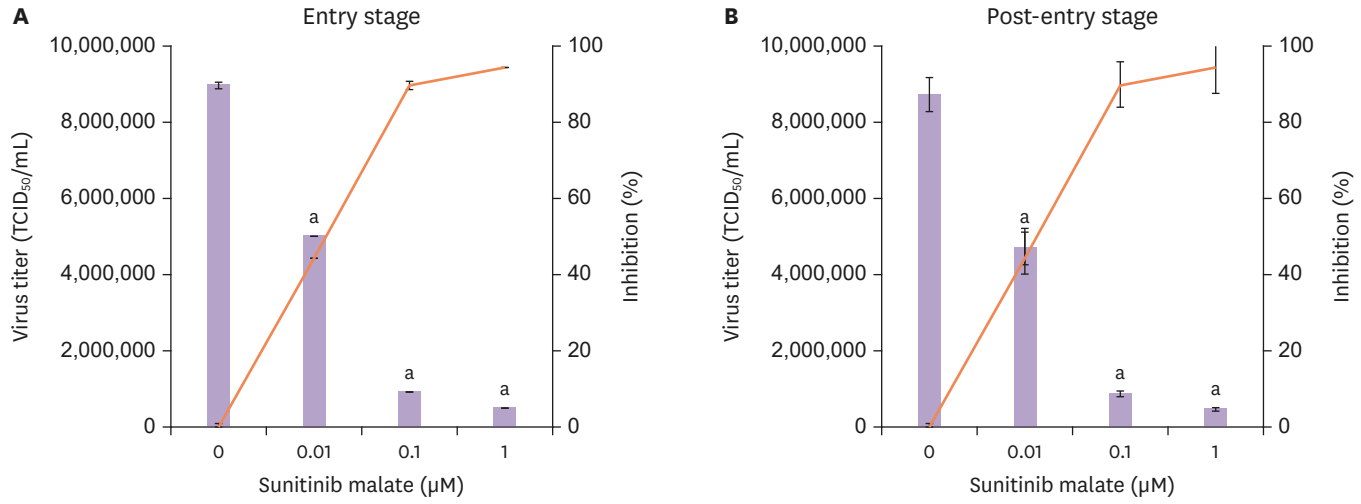

Figure 3. Time-of-addition and removal assay for analyzing antiviral action of sunitinib malate against ZIKV in BHK-21 cells.
The cell monolayer was infected with ZIKV strain PRVABC$_{59}$ (MOI = 0.05) and treated with sunitinib malate simultaneously (the entry-stage, A), or 1-hour post-infection (post-entry stage, B). After a 1-h incubation, the virus/the compound mixture was removed; the cell monolayer was washed with PBS. After an additional 120-h incubation, the supernatant from treated infected cells was harvested and serially diluted for determining virus yield using the TCID$_{50}$ assay (left y axis). The rate of virus yield inhibition was calculated based on the ratio of the loss in the titer of the treated group to un-treated group (right y axis).
[a]*P*-value <0.001 compared with un-treated infected cells.
ZIKV, Zika virus; BHK, baby hamster kidney; MOI, multiplicity of infection; TCID, tissue culture infectious dose.

reduced ZIKV RNA replication compared to mock-treatment (**Fig. 4C**). However, sunitinib malate treatment at post-stage increased the ratio of (+) RNA to (-) RNA in concentration-dependent manners (**Fig. 4F**), accumulating the large amounts of ZIKV (+) RNA and (-) RNA in infected cells. The results demonstrated the differential effect between treatment modes of sunitinib malate on ZIKV RNA replication at entry and post-entry stages.

To further explore the antiviral action of sunitinib malate on RNA encapsidation and virus release, the titer of intracellular infectious particles in mock and treated infected cells was determined using the TCID$_{50}$ assay (**Fig. 5**). Sunitinib malate treatment at entry stage meaningfully decreased the titer of intracellular infectious particles (**Fig. 5A**), as accompanied by the reduction of ZIKV RNA replication (**Fig. 4A-4C**). Interestingly, the treatment at post-stage caused a pointed increase in the titer of intracellular infectious particles by 0.01 and 0.1 μM sunitinib malate, but a substantial decrease in the titer of intracellular infectious particles by 1 μM sunitinib malate (**Fig. 5B**). Thus, sunitinib malate treatment at post-stage could interfere the release of the new viruses by the concentrations of 0.01 and 0.1 μM, and impede the RNA encapsidation (the assembly of the new viruses) by the concentration of 1 μM, as associated with accumulating the large amount of ZIKV (+) RNA and (-) RNA in infected cells (**Fig. 4D-4F**).

DISCUSSION

The study demonstrated anti-ZIKV activity of sunitinib malate in BHK-21 cells, which concentration-dependently reduced the level of ZIKV-induced CPE, the expression of viral proteins, and ZIKV yield in vitro (**Figs. 1**, **2**). Sunitinib malate processed the IC$_{50}$ value of 0.015 ± 0.002 μM on virus yield, and the selectivity index of greater than 100 against ZIKV infection, respectively (**Fig. 3**). Previous reports indicated the effective antiviral activity of sunitinib malate against many kinds of virus infections, such as SARS-CoV pseudovirus

https://doi.org/10.3947/ic.2021.0111

ic Infection & Chemotherapy

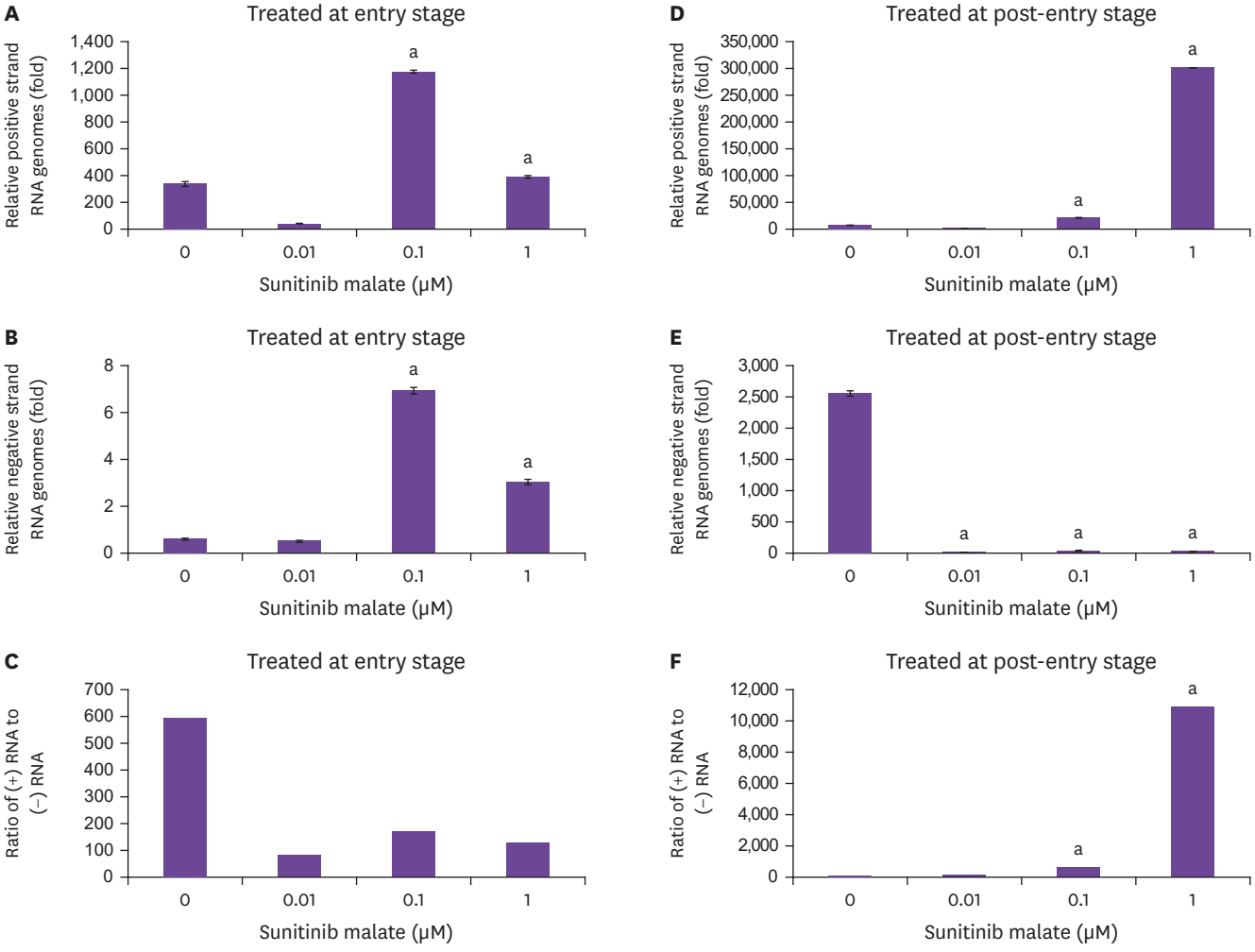

Figure 4. Effect of sunitinib malate treatment at entry and post-entry stages on ZIKV RNA replication in infected cells.
The cell monolayer was infected with ZIKV strain $PRVABC_{59}$ (MOI = 0.05) and treated with sunitinib malate simultaneously (the entry-stage, A-C), or 1 h post-infection (post-entry stage, D-F). After a 1-h incubation in cell-cultured wells, the virus/the compound mixture was removed; the cell monolayer was washed with PBS. After an additional 36-h incubation, the treated/infected cells were washed, harvested, and then lysed for total RNA extraction using using PureLink Mini Total RNA Purification Kit. Relative levels of ZIKV positive-strand RNA genomes (A, D) and negative-sense replicative RNA intermediates (B, E) in (un-) treated infected cells were determined by real-time RT-PCR assay. Finally, the ratio of (+) RNA to (-) RNA was computed (C, F).
[a]*P*-value <0.001 compared with un-treated infected cells.
ZIKV, Zika virus; MOI, multiplicity of infection; PBS, phosphate-buffered saline.

infection at an IC50 of 1 μM, SARS-CoV-2 pseudovirus infection at an IC_{50} of 0.33 μM [23], HCV pseudoparticles at an IC50 of 0.87 ± 0.178 μM, HCV cell culture system at an IC_{50} of 0.67 ± 0.18 μM [26], DENV2 at an IC_{50} of 0.51 μM, and Ebola virus at an IC_{50} of 0.51 μM of 0.47 μM [21], respectively. Therefore, our results revealed that sunitinib malate, a broad-spectrum antiviral agent, also exhibited the potent antiviral efficacy against ZIKV.

The study revealed antiviral mechanism of sunitinib malate at the entry and post-entry stages of ZIKV replication *in vitro* (**Fig. 3**), with the IC_{50} values of 0.011 ± 0.002 at entry stage, and 0.009 ± 0.001 at post-entry stage, respectively. Results demonstrated that sunitinib malate had multiple antiviral actions during the entry and post-entry stages of ZIKV replication. Relative levels of intracellular ZIKV (+) RNA and (-) RNA by real-time RT-PCR indicated that sunitinib malate treatment at post-entry stage caused a concentration-dependent increase in the levels of ZIKV (+) RNA and (-) RNA in infected cells, along with enlarging the ratio

https://doi.org/10.3947/ic.2021.0111

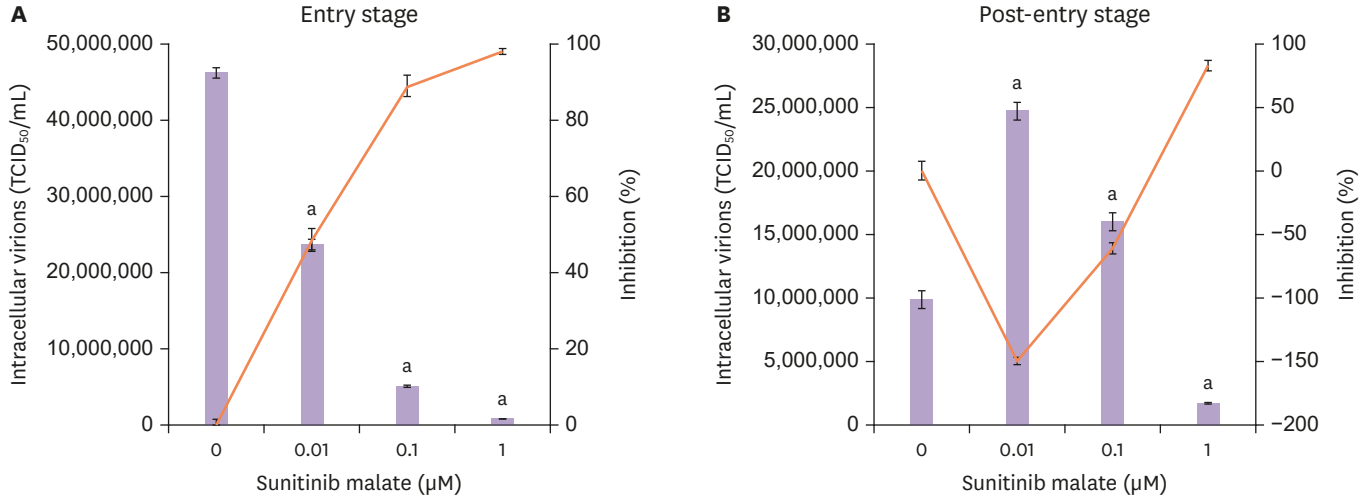

Figure 5. Effect of sunitinib malate treatment at entry and post-entry stages on intracellular virion production in ZIKV-infected cells.
The cell monolayer was infected with ZIKV strain PRVABC$_5$9 (MOI = 0.05) and treated with sunitinib malate simultaneously (the entry-stage, A), or 1 h post-infection (post-entry stage, B). After a 1-h incubation, the virus/the compound mixture was removed; the cell monolayer was washed with PBS. After an additional 72-h incubation, the treated/infected cells were washed, harvested, and then lysed by three freeze-thaw cycles. The titer of intracellular infectious particles was determined by $TCID_{50}$ assay (left y axis). The rate of virus yield inhibition was calculated based on the ratio of the loss in the titer of the treated group to un-treated group (right y axis).
[a]*P*-value <0.001 compared with un-treated infected cells.
ZIKV, Zika virus; MOI, multiplicity of infection; TCID, tissue culture infectious dose.

of (+) RNA to (-) RNA (**Fig. 4D-4F**). Meanwhile, the treatment at post-stage caused a pointed increase in the titer of intracellular infectious particles by 0.01 and 0.1 μM sunitinib malate, but a substantial decrease in the titer of intracellular infectious particles by1 μM sunitinib malate (**Fig. 5B**). The results suggested that sunitinib malate treatment at post-stage might inhibit the release of the new viruses and the assembly of the new viruses, which as associated with accumulating the large amount of ZIKV (+) RNA and (-) RNA in infected cells (**Fig. 4D-4F**). In the other hand, sunitinib malate treatment at entry stage significantly reduced the levels of ZIKV RNA replication with the reduction of (+) RNA to (-) RNA ratio and the production of new intracellular infectious particles in infected cells (**Figs. 4A-4C**, **5A**). The assays of virus yield, (+) RNA and (-) RNA, and intracellular infectious particles demonstrated the differential effect between treatment modes of sunitinib malate on ZIKV RNA replication at entry and post-entry stages. Since sunitinib malate distinctively inhibited AP-2-associated protein kinase 1 (AAK1) and cyclin G-associated kinase (GAK) with the regulation in endocytic and secretory pathways. Thus, the results implied that sunitinib malate specifically impede the endocytic and secretory pathways for ZIKV entry, assembly and release. Anti-ZIKV actions on the stages of entry and infectious virus production by sunitinib malate were consistent with the antiviral actions of sunitinib malate against many viruses, including HCV, DENV, Ebola, SARS-CoV and SARS-CoV-2. Such antiviral actions were associated with sunitinib-mediated inhibition of AAK1 and GAK activity [21, 23, 26].

The study discovered the antiviral potential of sunitinib malate against ZIKV infection, and provided the information for the development of sunitinib malate as a broad-spectrum antiviral agent. The study demonstrated a repurposed, host-targeted approach to identify potential antiviral drugs for treating emerging and global viral diseases. Drug repurposing, exhibiting known mechanisms and clinical trials of approved drugs, accelerates the clinical testing for treating emerging viruses with repurposed drugs.

https://doi.org/10.3947/ic.2021.0111

REFERENCES

1. Lindenbach BD, Thiel HJ, Rice CM. Flaviviridae: the viruses and their replication. In: Knipe DM, Howley PM, Griffin DE, Lamb RA, Martin MA, Roizman B, Straus SE, eds. Fields Virology, 5th ed. Philadelphia, PA: Lippincott Williams & Wilkins; 2006;1101-52.
2. Pan American Health Organization (PAHO), World Health Organization (WHO). Zika - Epidemiological update. 17 November 2016. Available at: http://www.paho.org/hq/index.php?option=com_docman&task=doc_view&Itemid=270&gid=36943&lang=en. Accessed 17 November 2016.
3. Duffy MR, Chen TH, Hancock WT, Powers AM, Kool JL, Lanciotti RS, Pretrick M, Marfel M, Holzbauer S, Dubray C, Guillaumot L, Griggs A, Bel M, Lambert AJ, Laven J, Kosoy O, Panella A, Biggerstaff BJ, Fischer M, Hayes EB. Zika virus outbreak on Yap Island, Federated States of Micronesia. N Engl J Med 2009;360:2536-43.
PUBMED | CROSSREF
4. Lanciotti RS, Kosoy OL, Laven JJ, Velez JO, Lambert AJ, Johnson AJ, Stanfield SM, Duffy MR. Genetic and serologic properties of Zika virus associated with an epidemic, Yap State, Micronesia, 2007. Emerg Infect Dis 2008;14:1232-9.
PUBMED | CROSSREF
5. Calvet G, Aguiar RS, Melo ASO, Sampaio SA, de Filippis I, Fabri A, Araujo ESM, de Sequeira PC, de Mendonça MCL, de Oliveira L, Tschoeke DA, Schrago CG, Thompson FL, Brasil P, Dos Santos FB, Nogueira RMR, Tanuri A, de Filippis AMB. Detection and sequencing of Zika virus from amniotic fluid of fetuses with microcephaly in Brazil: a case study. Lancet Infect Dis 2016;16:653-60.
PUBMED | CROSSREF
6. World Health Organization (WHO). WHO statement on the first meeting of the International Health Regulations 2005 (IHR 2005) Emergency Committee on Zika virus and observed increase in neurological disorders and neonatal malformations. Available at: http://www.who.int/mediacentre/news/statements/2016/1st-emergency-committee-zika/en/. Accessed 1 February 2016.
7. Fauci AS, Morens DM. Zika virus in the Americas--Yet another arbovirus threat. N Engl J Med 2016;374:601-4.
PUBMED | CROSSREF
8. Lessler J, Chaisson LH, Kucirka LM, Bi Q, Grantz K, Salje H, Carcelen AC, Ott CT, Sheffield JS, Ferguson NM, Cummings DA, Metcalf CJ, Rodriguez-Barraquer I. Assessing the global threat from Zika virus. Science 2016;353:aaf8160.
PUBMED | CROSSREF
9. Zhu Z, Chan JF, Tee KM, Choi GK, Lau SK, Woo PC, Tse H, Yuen KY. Comparative genomic analysis of pre-epidemic and epidemic Zika virus strains for virological factors potentially associated with the rapidly expanding epidemic. Emerg Microbes Infect 2016;5:e22.
PUBMED | CROSSREF
10. Yu Y, Deng YQ, Zou P, Wang Q, Dai Y, Yu F, Du L, Zhang NN, Tian M, Hao JN, Meng Y, Li Y, Zhou X, Fuk-Woo Chan J, Yuen KY, Qin CF, Jiang S, Lu L. A peptide-based viral inactivator inhibits Zika virus infection in pregnant mice and fetuses. Nat Commun 2017;8:15672.
PUBMED | CROSSREF
11. Yuan S, Chan JF, den-Haan H, Chik KK, Zhang AJ, Chan CC, Poon VK, Yip CC, Mak WW, Zhu Z, Zou Z, Tee KM, Cai JP, Chan KH, de la Peña J, Pérez-Sánchez H, Cerón-Carrasco JP, Yuen KY. Structure-based discovery of clinically approved drugs as Zika virus NS2B-NS3 protease inhibitors that potently inhibit Zika virus infection in vitro and in vivo. Antiviral Res 2017;145:33-43.
PUBMED | CROSSREF
12. Chan JF, Chik KK, Yuan S, Yip CC, Zhu Z, Tee KM, Tsang JO, Chan CC, Poon VK, Lu G, Zhang AJ, Lai KK, Chan KH, Kao RY, Yuen KY. Novel antiviral activity and mechanism of bromocriptine as a Zika virus NS2B-NS3 protease inhibitor. Antiviral Res 2017;141:29-37.
PUBMED | CROSSREF
13. Yuan J, Yu J, Huang Y, He Z, Luo J, Wu Y, Zheng Y, Wu J, Zhu X, Wang H, Li M. Antibiotic fidaxomicin is an RdRp inhibitor as a potential new therapeutic agent against Zika virus. BMC Med 2020;18:204.
PUBMED | CROSSREF
14. Adams VR, Leggas M. Sunitinib malate for the treatment of metastatic renal cell carcinoma and gastrointestinal stromal tumors. Clin Ther 2007;29:1338-53.
PUBMED | CROSSREF
15. Schor S, Einav S. Repurposing of kinase inhibitors as broad-spectrum antiviral drugs. DNA Cell Biol 2018;37:63-9.
PUBMED | CROSSREF

16. Schleiss M, Eickhoff J, Auerochs S, Leis M, Abele S, Rechter S, Choi Y, Anderson J, Scott G, Rawlinson W, Michel D, Ensminger S, Klebl B, Stamminger T, Marschall M. Protein kinase inhibitors of the quinazoline class exert anti-cytomegaloviral activity in vitro and in vivo. Antiviral Res 2008;79:49-61.
PUBMED | CROSSREF

17. Lupberger J, Zeisel MB, Xiao F, Thumann C, Fofana I, Zona L, Davis C, Mee CJ, Turek M, Gorke S, Royer C, Fischer B, Zahid MN, Lavillette D, Fresquet J, Cosset FL, Rothenberg SM, Pietschmann T, Patel AH, Pessaux P, Doffoël M, Raffelsberger W, Poch O, McKeating JA, Brino L, Baumert TF. EGFR and EphA2 are host factors for hepatitis C virus entry and possible targets for antiviral therapy. Nat Med 2011;17:589-95.
PUBMED | CROSSREF

18. García M, Cooper A, Shi W, Bornmann W, Carrion R, Kalman D, Nabel GJ. Productive replication of Ebola virus is regulated by the c-Abl1 tyrosine kinase. Sci Transl Med 2012;4:123ra24.
PUBMED | CROSSREF

19. Clark MJ, Miduturu C, Schmidt AG, Zhu X, Pitts JD, Wang J, Potisopon S, Zhang J, Wojciechowski A, Hann Chu JJ, Gray NS, Yang PL. GNF-2 inhibits Dengue virus by targeting Abl kinases and the viral E protein. Cell Chem Biol 2016;23:443-52.
PUBMED | CROSSREF

20. Dyall J, Coleman CM, Hart BJ, Venkataraman T, Holbrook MR, Kindrachuk J, Johnson RF, Olinger GG Jr, Jahrling PB, Laidlaw M, Johansen LM, Lear-Rooney CM, Glass PJ, Hensley LE, Frieman MB. Repurposing of clinically developed drugs for treatment of Middle East respiratory syndrome coronavirus infection. Antimicrob Agents Chemother 2014;58:4885-93.
PUBMED | CROSSREF

21. Bekerman E, Neveu G, Shulla A, Brannan J, Pu SY, Wang S, Xiao F, Barouch-Bentov R, Bakken RR, Mateo R, Govero J, Nagamine CM, Diamond MS, De Jonghe S, Herdewijn P, Dye JM, Randall G, Einav S. Anticancer kinase inhibitors impair intracellular viral trafficking and exert broad-spectrum antiviral effects. J Clin Invest 2017;127:1338-52.
PUBMED | CROSSREF

22. Weisberg E, Parent A, Yang PL, Sattler M, Liu Q, Liu Q, Wang J, Meng C, Buhrlage SJ, Gray N, Griffin JD. Repurposing of kinase inhibitors for treatment of COVID-19. Pharm Res 2020;37:167.
PUBMED | CROSSREF

23. Wang PG, Tang DJ, Hua Z, Wang Z, An J. Sunitinib reduces the infection of SARS-CoV, MERS-CoV and SARS-CoV-2 partially by inhibiting AP2M1 phosphorylation. Cell Discov 2020;6:71.
PUBMED | CROSSREF

24. Weng JR, Lin CS, Lai HC, Lin YP, Wang CY, Tsai YC, Wu KC, Huang SH, Lin CW. Antiviral activity of Sambucus FormosanaNakai ethanol extract and related phenolic acid constituents against human coronavirus NL63. Virus Res 2019;273:197767.
PUBMED | CROSSREF

25. Lu CY, Lin CS, Lai HC, Yu YW, Liao CY, Su WC, Ko BH, Chang YS, Huang SH, Lin CW. The rescue and characterization of recombinant, microcephaly-associated Zika viruses as single-round infectious particles. Viruses 2019;11:1005.
PUBMED | CROSSREF

26. Neveu G, Ziv-Av A, Barouch-Bentov R, Berkerman E, Mulholland J, Einav S. AP-2-associated protein kinase 1 and cyclin G-associated kinase regulate hepatitis C virus entry and are potential drug targets. J Virol 2015;89:4387-404.
PUBMED | CROSSREF